# First-principles study of the pressure dependence of the structural and vibrational properties of the ternary metal hydride $Ca_2RuH_6$

Latévi Max Lawson Daku* and Hans Hagemann
*Département de chimie physique, Université de Genève, 30 quai Ernest-Ansermet, CH-1211 Genève 4, Switzerland*
(Received 18 February 2007; revised manuscript received 11 May 2007; published 26 July 2007)

The influence of pressure on the structural and vibrational properties of $Ca_2RuH_6$ has been investigated using periodic density functional theory calculations performed at the local density approximation (LDA) and generalized gradient approximation (GGA) levels. At ambient pressure, the calculated structure and vibrational frequencies are in satisfactory agreement with experimental data. The calculated *P-V* curves could be fitted with the Vinet equation of state, yielding $B_0$=67.6 and $B_0$=58.5 GPa at the LDA and GGA levels, respectively, and $B_0'$=4.0 at both theoretical levels. The unit cell parameter is found to decrease faster with increasing pressure than the Ru–H bond length. The calculated pressure dependence of the vibrational frequencies agrees well with experiment for $\nu_5(T_{2g})$ but not for $\nu_9(A_{1g})$.

DOI: 10.1103/PhysRevB.76.014118 PACS number(s): 71.15.Mb, 62.20.−x, 63.20.−e

## I. INTRODUCTION

Complex metal hydrides are actively considered as potential hydrogen storage materials.[1] For instance, the compound $Mg_2FeH_6$ attracts much attention because of its very high volume and mass storage efficiency: 150 g/l and 5.4 wt %. It belongs to a family of ternary hydrides $M_2M'H_6$ ($M$=Mg,Ca,Sr,Ba,Eu,Sm; $M'$=Fe,Ru,Os) with the same $K_2PtCl_6$ structure.[2] In this context, it is of more than fundamental interest to gain more insight into the properties of these ternary transition metal hydrides. The electronic structure and stability of several of these $M_2M'H_6$ hydrides have been recently investigated by Halilov *et al.* within density functional theory (DFT).[3] Their results show that these hydrides are ionic materials made of molecular $[M'H_6]^{4-}$ units stabilized by the Madelung field and that they are very stable. This last feature is actually shared by most metal hydrides which are potential candidates for hydrogen storage so that much effort is being made for destabilizing metal hydrides by mixing them with other compounds.[4] From the experimental point of view, vibrational spectroscopies provide a convenient means to investigate the $M_2M'H_6$ hydrides and especially the strength of the $M'$–H bond. We have studied in the past Raman spectra of some members of this family of compounds,[5] completing previous infrared studies.[2]

If one considers the issue of hydrogen storage in the solid state, one has to take into account the external variables temperature and pressure. For the direct investigation of systems under pressure, vibrational spectroscopies often prove to remain methods of choice. In this regard, a pressure-dependent Raman study on $M_2RuH_6$ ($M$=Ca,Sr,Eu) has been recently reported.[6] In the present study, we aim to theoretically study the effect of pressure on one of these compounds, namely, $Ca_2RuH_6$, using periodical calculations within DFT.[7–9] More specifically, we will investigate the pressure dependence of the structure and of the vibrational properties of $Ca_2RuH_6$, and will compare our results with experimentally available data.[6] Prior to this, we will discuss the properties of the title compound at ambient pressure. This will be done on the basis of the results of calculations carried out at zero pressure and on the basis of experimental data that will include the results of new Raman spectroscopy measurements performed at ambient pressure on $Ca_2RuH_6$ and $Ca_2RuD_6$ samples.

## II. EXPERIMENTAL AND COMPUTATIONAL DETAILS

The details of the procedure used for the preparation of the samples of $Ca_2RuH_6$ and $Ca_2RuD_6$ and those of the experimental setup used for the Raman spectroscopy measurements have been reported elsewhere.[5] The calculations were carried out within the local density approximation[10] (LDA) and generalized gradient approximation (GGA),[11,12] using the ABINIT code,[13–15] which is based on pseudopotentials and plane waves. It relies on an efficient fast Fourier transform algorithm[16] for the conversion of wave functions between real and reciprocal spaces, on the adaptation to a fixed potential of the band-by-band conjugate gradient method[17] and on a potential-based conjugate-gradient algorithm for the determination of the self-consistent potential.[18] We used fully nonlocal Troullier-Martins pseudopotentials[19] generated thanks to the FHI98PP code.[20] Nonlinear core corrections were applied to calcium.[21] In order to determine the optimal integration conditions, geometry optimizations were performed using the Monkhorst-Pack[22] grids $2\times2\times2$, $4\times4\times4$, and $6\times6\times6$ in combination with values of the plane wave kinetic energy cutoff which have been varied between 10 and 45 hartree with an increment of 5 hartree. The chosen conditions correspond to an energy cutoff of 30 hartree and the $4\times4\times4$ Monkhorst-Pack grid and enabled convergence to within 1 mhartree for the total energy, within $10^{-3}$ Å for the cell parameter $a$, and within 0.05 GPa for the pressure. Phonons were calculated at the center of the Brillouin zone within density-functional perturbation theory: the technical details on the computation of responses to atomic displacements and homogeneous electric fields can be found in Ref. 23, while Ref. 24 presents the subsequent computation of dynamical matrices, Born effective charges, dielectric permittivity tensors, and interatomic force constants. The symmetry analysis of the vibrational modes was performed with the ABINIT utility "get_irrep.py," which makes use of the data available on the Bilbao Crystallographic Server.[25] All calcu-

 

TABLE I. Cell parameter $a$ (Å), H position $x_H$, Ru-H distance ($a \times x_H$; in Å), and vibrational frequencies $\nu$ ($cm^{-1}$) calculated at zero pressure for $Ca_2RuH_6$. Known experimental values at ambient pressure are also reported for comparison. Numbers in brackets are vibrational frequencies calculated ($P=0$) or measured (ambient pressure) for $Ca_2RuD_6$.

| LDA | | GGA | | Expt. | |
|---|---|---|---|---|---|
| [a] | 7.084 | [a] | 7.253 | [a] | 7.229[a] |
| $x_H$ | 0.2395 | $x_H$ | 0.2373 | | |
| Ru-H | 1.697 | Ru-H | 1.721 | | |
| $\nu_1(T_{1u})$ | 203 [202] | $\nu_1(T_{1u})$ | 185 [184] | | |
| $\nu_2(T_{2g})$ | 211 [211] | $\nu_2(T_{2g})$ | 198 [198] | $\nu_2(T_{2g})$ | 194[b] [196[b]] |
| $\nu_3(T_{1g})$ | 541 [383] | $\nu_3(T_{1g})$ | 457 [323] | | |
| $\nu_5(T_{2g})$ | 843 [596] | $\nu_4(T_{2u})$ | 810 [573] | | |
| $\nu_4(T_{2u})$ | 840 [596] | $\nu_5(T_{2g})$ | 825 [584] | $\nu_5(T_{2g})$ | 875[b] [620[b]] |
| $\nu_6(T_{1u})$ | 888 [635] | $\nu_6(T_{1u})$ | 858 [614] | $\nu_6(T_{1u})$ | 896[c] [646[c]] |
| $\nu_7(T_{1u})$ | 1656 [1183] | $\nu_7(T_{1u})$ | 1585 [1132] | $\nu_7(T_{1u})$ | 1564[c] [1128[c]] |
| $\nu_8(E_g)$ | 1852 [1310] | $\nu_8(E_g)$ | 1772 [1253] | $\nu_8(E_g)$ | 1754[d] [1274[d]] |
| $\nu_9(A_{1g})$ | 1870 [1323] | $\nu_9(A_{1g})$ | 1801 [1274] | $\nu_9(A_{1g})$ | 1833[b] [1315[b]] |

[a]Taken from Ref. 26.
[b]This work. The resolution of the Raman spectra is 3 $cm^{-1}$.
[c]Taken from Ref. 5.
[d]Taken from Ref. 6.

lations were performed with the symmetry fixed to the cubic space group $Fm\bar{3}m \equiv O_h^5$ (number 225): Ca is on site 8$c$ (1/4,1/4,1/4), Ru on site 4$a$ (0,0,0), and H on site 24$e$ ($x_H$,0,0). The phonon calculations confirmed that this structure is stable.

## III. RESULTS AND DISCUSSION

The cubic $Fm\bar{3}m$ structure of the title compound is fully determined by the lattice constant $a$ and the H position $x_H$. Table I summarizes the LDA and GGA results obtained at zero pressure for the relaxed structure and the vibrational properties of $Ca_2RuH_6$.

At the LDA level, the optimized cell parameter value of 7.084 Å is about 3% lower than the experimental value of 7.229 Å.[26] This stems from the well-known fact that LDA tends to overestimate bonding energies and to underestimate interatomic distances. The agreement with experiment improves on passing to the GGA level which gives a cell parameter value of 7.253 Å. At both the LDA and GGA levels, the optimized Ru–H bond lengths are close to the value of 1.675 Å estimated for $Ca_2RuH_6$ using the Badger's rule.[5] The vibrational frequencies above 800 $cm^{-1}$ correspond to vibrations of the $RuH_6$ octahedron and, besides the IR and Raman inactive $T_{2u}$ mode, they have been observed by IR and Raman spectroscopies (see Table I). The classification of the vibrational modes of $Ca_2RuH_6$ is given Table II.

For the observed internal modes, the isotope shift for the same mode in $Ca_2RuH_6$ and $Ca_2RuD_6$ obeys the relation $\nu^H/\nu^D \approx 1.4$, as expected. These experimental data are well reproduced at the LDA and GGA levels, the GGA giving an overall better agreement. This makes us confident about the frequencies and isotopic shifts ($\nu^H/\nu^D \approx 1.4$) predicted for the Ru-H bending $\nu_4(T_{2u})$ and the librational $\nu_3(T_{1g})$ modes which both are Raman and IR inactive. As shown in Table I, our new Raman spectroscopy measurements on $Ca_2RuH_6$ allowed the identification of the band associated with the optical translational mode of $T_{2g}$ symmetry, at $\nu_2(T_{2g}) = 194$ $cm^{-1}$. No isotopic shift is observed for this mode: This is in agreement with the fact that this mode only involves the motion of the $Ca^{2+}$ cations. Our experimental finding for $\nu_2(T_{2g})$ is confirmed by the results of the DFT calculations, an excellent agreement between experiment and theory being observed for the GGA results. At the GGA level, the $T_{1u}$ optical translational mode is predicted at $\nu_1(T_{1u}) = 185$ $cm^{-1}$, and at 203 $cm^{-1}$ at the LDA level. Note that, excepted for $Mg_2FeH_6$ which has been studied by inelastic neutron scattering (INS) spectroscopy,[27] none of the two optical translational modes has been reported so far for any of the other $M_2M'H_6$ ternary metal hydrides. Let us also add that *ab initio* studies of vibrational properties of such hydrides remain scarce. In their theoretical investigation of the electronic structure and stability of ternary metal hydrides carried out within the LDA using the linearized augmented plane wave method, Halilov *et al.* performed a partial struc-

TABLE II. Vibrational modes of $Ca_2RuH_6$: symmetries and labeling used for the associated frequencies. $T_{1u}$ modes are IR active; $A_{1g}$, $E_g$, and $T_{2g}$ modes are Raman active; $T_{2u}$ and $T_{1g}$ modes are IR and Raman inactive.

| | | |
|---|---|---|
| Ru-H stretching modes | $A_{1g} \oplus E_g \oplus T_{1u}$ | $\nu_9(A_{1g})$, $\nu_8(E_g)$, $\nu_7(T_{1u})$ |
| Ru-H bending modes | $T_{1u} \oplus T_{2g} \oplus T_{2u}$ | $\nu_6(T_{1u})$, $\nu_5(T_{2g})$, $\nu_4(T_{2u})$ |
| Librational mode | $T_{1g}$ | $\nu_3(T_{1g})$ |
| Optical translational modes | $T_{2g} \oplus T_{1u}$ | $\nu_2(T_{2g})$, $\nu_1(T_{1u})$ |

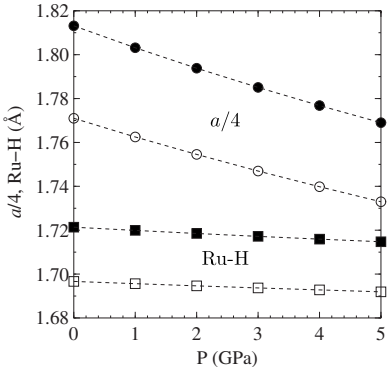


FIG. 1. Pressure dependence of the cell parameter $a/4$ (circles) and of the Ru–H bond length (squares): LDA (open symbols) and GGA results (filled symbols); dashed lines serve as guides for eyes.

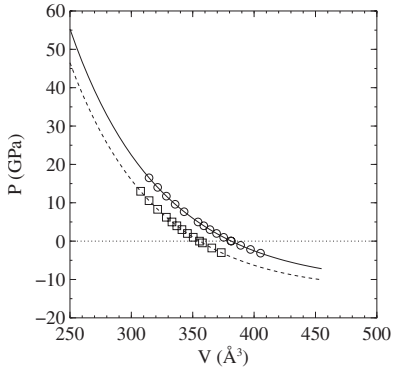


FIG. 2. Calculated LDA (squares) and GGA (circles) $P$-$V$ curves at $T=0$ K fitted by the Vinet EOS (LDA, dashed line; GGA, solid line).

tural relaxation with the unit cell parameter $a$ fixed at their experimental values. For $Ca_2RuH_6$, they obtained a Ru–H bond length of 1.705 Å and reported a totally symmetric stretching frequency of $\nu_9(A_{1g})=1837$ cm$^{-1}$,[3] which is in good agreement with our LDA results. In summary, we have provided a detailed description of the vibrational spectrum of $Ca_2RuH_6$ at ambient pressure on the basis of our DFT results, while extending the number of observed features to the Raman active $T_{2g}$ translational mode. INS spectroscopy would allow the observation of all vibrational modes and thus would help further assess the performance of the DFT methods for the description of the complete vibrational spectrum. Despite the lack of such data, the overall very good agreement between our theoretical results and the available experimental data shows that DFT can be reliably used to study the pressure dependence of the properties of $Ca_2RuH_6$.

In order to investigate the influence of pressure on the structure of $Ca_2RuH_6$, its geometry has been fully optimized with specified target pressure of up to 5 GPa, which corresponds to the experimentally investigated pressure range.[6] Figure 1 summarizes the resulting theoretical pressure dependences of the Ru–H bond length and of the cell parameter $a/4$. Both LDA and GGA calculations predict the same behavior: the two parameters, $a/4$ and the Ru–H bond length, are decreasing functions of the pressure. However, it is important to note that the volume of the unit cell decreases faster than the volume of the $RuH_6$ octahedron. A similar behavior is observed experimentally with "chemical pressure:" in the solid solutions $Ca_{2-x}Eu_xRuH_6$,[28] the lattice parameter changes from 7.227 to 7.566 Å (i.e., by more than 4%), while the Ru-H distance is estimated to increase only by $\sim 1\%$.[5]

Figure 2 shows the calculated LDA and GGA $P$-$V$ curves for a wider pressure range than in Fig. 1. These curves have been obtained by relaxing the structure for fixed values of the cell parameter $a$ (i.e., for fixed volumes $V=a^3$) and by recording the resulting pressure. The smallest $a$ value was chosen such that the Ru-H distance remains smaller than $a/4$ to avoid complications due to interpenetrating octahedra in the structure. The curves have been fitted using the Vinet equation of state:[29]

$$P=[3B_0(1-x)/x^2]\exp[\eta(1-x)], \tag{1}$$

with

$$x=\left(\frac{V}{V_0}\right)^{1/3}, \tag{2}$$

$$\eta=\frac{3}{2}(B_0'-1). \tag{3}$$

$V_0$ is the zero-pressure volume, and $B_0$ and $B_0'$ are the bulk modulus and its pressure derivative, respectively. It can be seen in Fig. 2 that the fits are very good; the results are summarized in Table III. The LDA and GGA $B_0$ values are comparable, the LDA value being about 16% higher than the GGA value as expected. As for the pressure derivative of the bulk modulus, the fits give $B_0'=4.0$ at both theoretical levels.

The calculated LDA and GGA pressure dependences of the vibrational frequencies are shown in Fig. 3. In both cases, the pressure dependence is close to linear as experimentally observed for the $A_{1g}$ ($\nu_9$) and $T_{2g}$ ($\nu_5$) modes.[6] Experimentally, $\nu_9$ is shown to exhibit a strong pressure dependence ($[d\nu_9/dP]_{\text{expt}}=17.43$ cm$^{-1}$/GPa), which is more pronounced than the calculated behavior ($[d\nu_9/dP]_{\text{GGA}}=5.96$ cm$^{-1}$/GPa and $[d\nu_9/dP]_{\text{LDA}}=4.15$ cm$^{-1}$/GPa). On the other hand, the calculated pressure variation of $\nu_5$ shows a good agreement with the experimental behavior ($[d\nu_5/dP]_{\text{expt}}=9.49$ cm$^{-1}$/GPa, $[d\nu_5/dP]_{\text{GGA}}=11.44$ cm$^{-1}$/GPa, and $[d\nu_5/dP]_{\text{LDA}}=10.75$ cm$^{-1}$/GPa). As pointed out by Barsan *et al.*,[6] the stretching mode $\nu_9$ is more sensitive to anharmonicity than the lower frequency bending mode $\nu_5$.

The mode Grüneisen parameter $\gamma_i$ represents the volume dependence of the frequency $\nu_i$ of the $i$th vibrational mode of the lattice:

TABLE III. Equilibrium volume $V_0$ at $P=0$, bulk modulus $B_0$, and its derivative $B_0'$ with respect to pressure obtained from the fit of the $P$-$V$ curve by the Vinet equation of state (EOS) (Ref. 29).

| | $V_0$ (Å$^3$) | $B_0$ (GPa) | $B_0'$ |
|---|---|---|---|
| LDA | 355.5 | 67.6 | 4.0 |
| GGA | 381.4 | 58.5 | 4.0 |

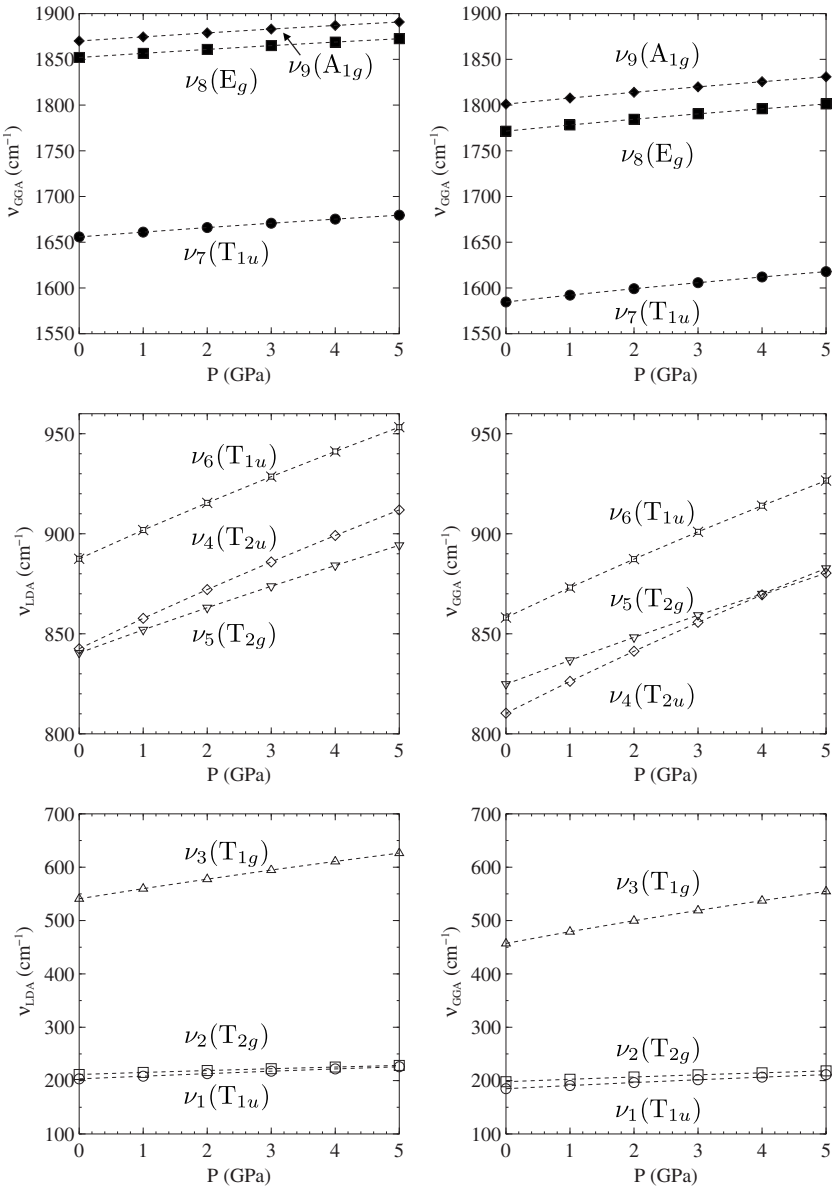


FIG. 3. LDA (left) and GGA (right) pressure dependences of the frequencies of the vibrational modes (dashed lines serve as guides for eyes).

$$\gamma_i = -\left.\frac{\partial \ln \nu_i}{\partial \ln V}\right|_0. \tag{4}$$

$$\gamma_i = B_0\left(\frac{\partial \ln \nu_i}{\partial P}\right), \tag{5}$$

Figure 4 shows the plots of log $\nu$ against log $V$ for the nine vibrational modes. One observes in each case a linear dependence which allows the determination of the mode Grüneisen parameters [Eq. (4)]. The calculated values are summarized in Table IV along with available experimental data. The LDA and GGA values are quite similar. The Grüneisen parameters for the Ru-H stretching modes, $\nu_i$ $(i=7,8,9)$, are much smaller than the other parameters. This behavior can be explained by the smaller variation of the Ru–H bond length with pressure as compared to the lattice parameter. The librational mode $\nu_3$ shows the largest Grüneisen parameter and this reflects the great sensitivity of this mode to the lattice dimensions.

For the analysis of their experimental data, because they do not know the pressure dependence of the volume, Barsan *et al.*[6] made use of the alternative form

where $B_0$ is the bulk modulus at atmospheric pressure. In order to determine the missing parameter $B_0$, they assumed that the frequencies depend linearly on the cell parameter,

$$\nu_i = \nu_{a,i}^0 + m_{a,i} \times a, \tag{6}$$

and likewise on the pressure

$$\nu_i = \nu_{P,i}^0 + m_{P,i} \times P. \tag{7}$$

Equating the two equations above gives the cell parameter as a linear function of $P$, thus leading for the bulk modulus to the formula below

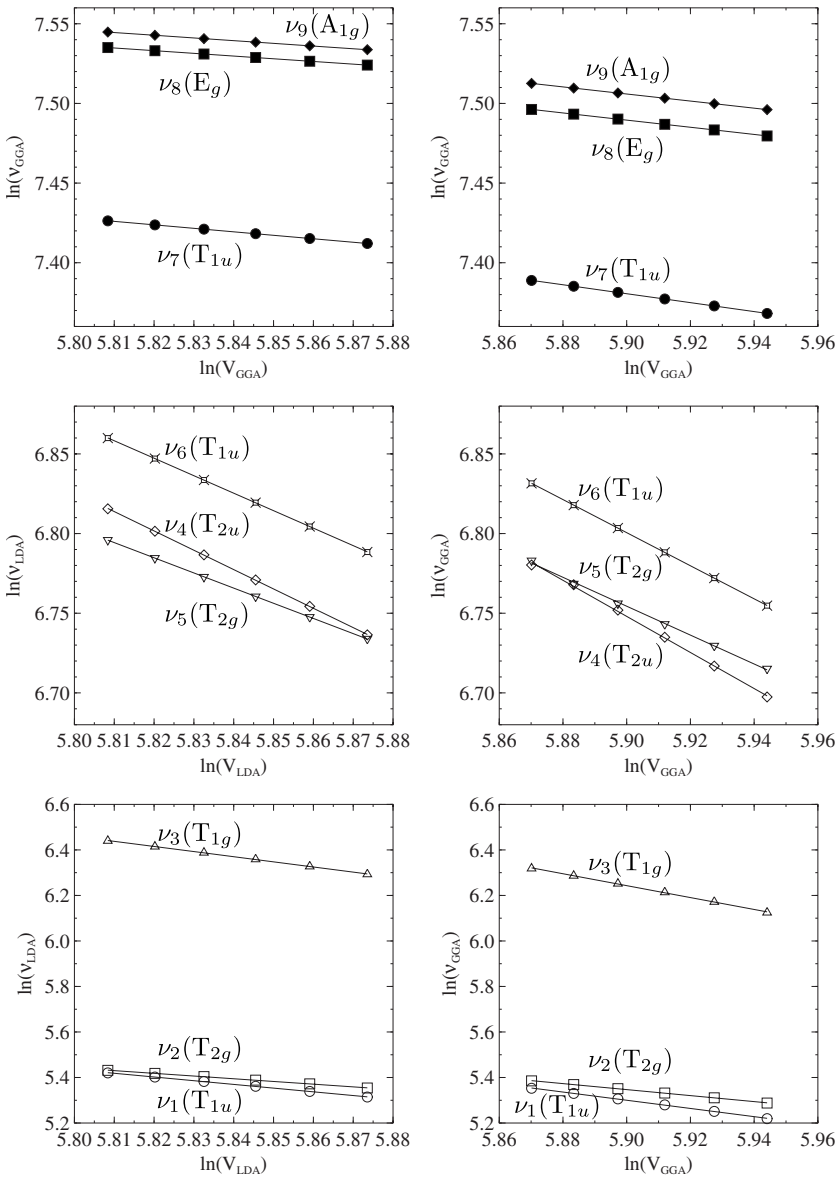


FIG. 4. Plot of the logarithms of the frequencies versus the logarithm of the cell volume, as obtained from the calculations at the LDA (left) and GGA (right) levels. The solid lines represent the least-squares fits to the data.

$$B_{0,i} = -\frac{\nu_{P,i}^0 - \nu_{a,i}^0}{3m_{P,i}}. \quad (8)$$

The numerical precision of this equation relies on the accuracy of the values of $\nu_{a,i}^0$ as determined from experiment. The $\nu_{a,i}^0$'s have been deduced from the values of the $\nu_i$'s for $a=7.227$ Å ($Ca_2RuH_6$), $a=7.566$ Å ($Eu_2RuH_6$), and $a=7.609$ Å ($Sr_2RuH_6$), extrapolated to $a=0$. Barsan *et al.* thus obtained $B_0$ values of $B_{0,9}=18.8$ and $B_{0,5}=17.4$ GPa.[6] These values are much smaller than those deduced from our DFT calculations using the Vinet equation of state (Table III). Using Eq. (8), we actually calculate even higher values of $B_0$: $B_{0,i}=77.7$ GPa at the LDA level, and $B_{0,i}=68.6$ GPa at the GGA level ($i=1,\ldots,9$). Note that this procedure implicitly averages the value of the bulk modulus over the pressure range of 0–5 GPa probed. These estimates thus remain in satisfactory agreement with the values obtained with the Vi-

TABLE IV. Calculated and available experimental values for the mode Grüneisen parameters $\gamma_i$ ($i=1-9$).

| | $\gamma_1(T_{1u})$ | $\gamma_2(T_{2g})$ | $\gamma_3(T_{1g})$ | $\gamma_4(T_{2u})$ | $\gamma_5(T_{2g})$ | $\gamma_6(T_{1u})$ | $\gamma_7(T_{1u})$ | $\gamma_8(E_g)$ | $\gamma_9(A_{1g})$ |
|---|---|---|---|---|---|---|---|---|---|
| LDA | 1.623 | 1.189 | 2.254 | 1.215 | 0.952 | 1.097 | 0.219 | 0.169 | 0.170 |
| GGA | 1.804 | 1.319 | 2.618 | 1.133 | 0.907 | 1.039 | 0.281 | 0.225 | 0.223 |
| Expt.[a] | | | | | 0.188 | | | | 0.178 |

[a]Reference 6.

net equation of state, and attest for the consistency and self-containedness of our results and for the reasonable accuracy which then can be achieved by making use of Eq. (8) for the determination of $B_0$.

In order to understand the large discrepancy observed between the theoretical and the experimental estimates of the bulk modulus, we must turn back to the procedure used by Barsan *et al.* for the analysis of their data. This procedure relies on the fact that, as we have shown above, the variations of the frequencies of the internal modes of the $RuH_6$ octahedron can effectively be used to quantify the pressure exerted on a given $M_2RuH_6$ compound and the concomitant change of its structural parameter $a$. While they could accurately measure the pressure dependence of the frequencies for $Ca_2RuH_6$, Barsan *et al.* did not know the pressure dependence of $a$ (which, in fact, would have allowed the direct determination of $B_0$) nor how to relate the observed frequency shifts to the pressure-induced variations of $a$. They therefore made the assumption of the linear dependencies of the frequencies on the cell parameter $a$ [Eq. (6)], which our results clearly show to be reasonable. Then, on the basis of the correlation between the vibrational wave numbers and the cell parameter $a$ observed for neat $M_2RuH_6$ hydrides,[2] they deduced the parameters entering in Eq. (6) from the knowledge of these frequencies for $Ca_2RuH_6$ ($a$=7.227 Å), $Eu_2RuH_6$ ($a$=7.566 Å), and $Sr_2RuH_6$ ($a$=7.609 Å). In doing this, they actually state that the simultaneous variations of the frequencies of the $[RuH_6]^{4-}$ complex and of the cell parameter achieved by applying an external pressure are the same as those obtained by playing with the counterion $M^{2+}$, thus implicitly assuming a complete equivalence between physical and chemical pressures. Indeed, within the chemical pressure picture as applied to these ternary metal hydrides, varying the nature of the dication $M^{2+}$—or equivalently its radius—helps mimic the effects of the external pressure in that it is an efficient means to control the structure hence the room available to the $RuH_6$ units.

This last assumption proves to be the cornerstone of the experimental determination of the bulk modulus. In order to test its validity, we have determined at the GGA level the relaxed Ru-H distance and the vibrational frequencies of $Ca_2RuH_6$ at values of the cell parameter $a$ that correspond to those of $Eu_2RuH_6$ and $Sr_2RuH_6$. They are reported in Table V along with available experimental values for $Eu_2RuH_6$ and $Sr_2RuH_6$, which they should match with, were the assumption valid.

In passing for $Ca_2RuH_6$ from its zero-pressure optimized structure (Table I) to those expanded structures (Table V), there is as expected a lengthening of the Ru–H bond, but by some ~0.01 Å only. This illustrates the previously noticed weak sensitivity of the Ru–H bond length to the dimension of the lattice. One also notes in Table V that the simulated expansions of the structure of $Ca_2RuH_6$ actually correspond to the application of negative hydrostatic pressures of about −6 GPa. However, using for $\nu_5(T_{2g})$ and $\nu_9(A_{1g})$ their experimental pressure dependences in $Ca_2RuH_6$ ($[d\nu_5/dP]_{expt}$ =9.49 $cm^{-1}$/GPa, $[d\nu_9/dP]_{expt}$=17.43 $cm^{-1}$/GPa)[6] and their measured frequencies in $M_2RuH_6$ ($M$=Ca,Eu,Sr; Tables I and V), one predicts estimates of the hydrostatic pressure of ≈−3 GPa. That is, the use of the chemical pressure image leads to a severe underestimation of the magnitude of the hydrostatic pressure by a factor of roughly 2. This clearly invalidates the above assumption that the chemical and the physical pressures may be equated. Furthermore, if one uses Eq. (8) with the vibrational frequencies $\nu_i$ ($i$=1,...,9) calculated for $Ca_2RuH_6$ in its zero-pressure structure ($a$=7.253 Å) and in its expanded structures ($a$ =7.566,7.609 Å), one obtains $B_{0,i}$=43.7 GPa ($i$=1,...,9), in reasonably good agreement with the bulk modulus of 58.5 GPA obtained at the GGA level with the Vinet equation of state.

TABLE V. GGA H positions $x_H$, Ru-H distances ($a \times x_H$; in Å), and vibrational frequencies $\nu$ ($cm^{-1}$) determined for $Ca_2RuH_6$ using values of the cell parameter $a$ (Å) that correspond to those of $Eu_2RuH_6$ and $Sr_2RuH_6$ at ambient pressure. Known ambient-pressure experimental values are also reported for $Eu_2RuH_6$ and $Sr_2RuH_6$.

| | $Ca_2RuH_6$ (GGA results) | | $Eu_2RuH_6$ | $Sr_2RuH_6$ |
|---|---|---|---|---|
| [a] | 7.566 | 7.609 | 7.566[a] | 7.609[a] |
| $x_H$ | 0.2290 | 0.2279 | ··· | ··· |
| Ru-H | 1.732 | 1.734 | ··· | 1.69[b] |
| $P$ | −5.8 | −6.3 | ··· | ··· |
| $\nu_1(T_{1u})$ | 137 | 130 | ··· | ··· |
| $\nu_2(T_{2g})$ | 162 | 157 | ··· | ··· |
| $\nu_3(T_{1g})$ | 278 | 251 | ··· | ··· |
| $\nu_4(T_{2u})$ | 694 | 680 | ··· | ··· |
| $\nu_5(T_{2g})$ | 742 | 732 | 840[c] | 850[c] |
| $\nu_6(T_{1u})$ | 750 | 736 | 878[d] | 880[d] |
| $\nu_7(T_{1u})$ | 1527 | 1519 | 1480[b] | 1482[b] |
| $\nu_8(E_g)$ | 1720 | 1713 | 1713[c] | 1731[c] |
| $\nu_9(A_{1g})$ | 1751 | 1744 | 1785[c] | 1782[c] |

[a]Taken from Ref. 2.
[b]Taken from Ref. 30.
[c]Taken from Ref. 6.
[d]Taken from Ref. 28.

Inspection of Tables I and V shows that the expansion of the structure of $Ca_2RuH_6$ gives rise to the expected decrease of the vibrational frequencies, which is more or less pronounced depending on the nature of the involved vibrational modes. Focusing on the internal modes which are those of particular interest to us here, the decrease amounts to ~50 $cm^{-1}$ for the stretching modes and to ~100 $cm^{-1}$ for the bending modes. Surprisingly, the frequencies thus obtained for the stretching modes in the $Ca_2RuH_6$ expanded structures are in good agreement with the experimental values reported for $Eu_2RuH_6$ and $Sr_2RuH_6$. Given that the Ru–H bonds lie parallel to the axes of the conventional cubic cell and that their lengths vary far less rapidly than the cell parameter $a$, this agreement actually suggests that, for sufficiently large $a$ values, the stretching modes become weakly sensitive to the room made available to the $RuH_6$ octahedra such that the frequencies of these modes in $M_2RuH_6$ compounds characterized by such large $a$ values may fall in the same ballpark. In contrast, the bending modes are more sen-

sitive to the space available to the $RuH_6$ units and are consequently predicted to be softer in the $Ca_2RuH_6$ expanded structures than in $Eu_2RuH_6$ and $Sr_2RuH_6$. Indeed, the room available to the $RuH_6$ octahedra is controlled by the ionic radius of the $M^{2+}$ cations that occupy the tetrahedral sites, and the radius of $Ca^{2+}$ is smaller than those of $Eu^{2+}$ and $Sr^{2+}$.

## IV. CONCLUDING REMARKS

Using periodic DFT calculations performed at both the LDA and GGA levels, we have achieved a consistent and fairly satisfactory description of the pressure dependence of the structural and vibrational properties of $Ca_2RuH_6$. The calculated zero-pressure structure and vibrational frequencies of $Ca_2RuH_6$ and $Ca_2RuD_6$ were thus found to be in very good agreement with available ambient-pressure data, the GGA giving the best overall agreement. In particular, these results helped confirm the identification from new ambient-pressure Raman spectroscopy measurements of the frequency of the optical translation mode of $T_{2g}$ symmetry at 194 $cm^{-1}$, while quantitatively reproducing the isotopic frequency shifts observed in passing from $Ca_2RuH_6$ to $Ca_2RuD_6$. The comparison of the calculated pressure dependences of the frequencies with the available experimental data shows a good agreement for the pressure dependence of the frequency of the $\nu_5(T_{2g})$ bending mode, but not for the pressure dependence of the frequency of the $\nu_9(A_{1g})$ stretching mode which, as noticed by Barsan *et al.*,[6] is more sensitive to anharmonicity. The fits of the calculated LDA and GGA *P-V* curves using the Vinet equation of state gave LDA and GGA $B_0$ values of 67.6 and 58.5 GPa, respectively, which do not support the experimental estimate of $B_0 \approx 18$ GPa.[6] This discrepancy cannot be explained by the temperature and zero-point phonon effects which typically account for the up to 20% overestimation of bulk moduli frequently observed in zero-temperature *ab initio* calculations of $B_0$.[31] The origin of this discrepancy could be traced to the fact that the equivalence between chemical and physical pressures assumed for the experimental determination of $B_0$ does not quantitatively hold for the ternary metal hydrides. A fair comparison between experiment and theory actually relies on an accurate experimental determination of the pressure dependence of the lattice parameter *a*. We expect that our results will stimulate such an experimental study, and we are working on taking anharmonic as well as temperature effects into account in the description of the investigated properties of $Ca_2RuH_6$.[32]

## ACKNOWLEDGMENTS

We thank Fabien Tran and Matthieu Verstraete for helpful discussions. This work has benefited from the financial support of the Swiss National Science Foundation.

*max.lawson@unige.ch

[1] L. Schlapbach and A. Züttel, Nature (London) **414**, 353 (2001).
[2] M. Kritikos and D. Noréus, J. Solid State Chem. **93**, 256 (1991).
[3] S. V. Halilov, D. J. Singh, M. Gupta, and R. Gupta, Phys. Rev. B **70**, 195117 (2004).
[4] S. V. Alapati, J. K. Johnson, and D. S. Sholl, Phys. Chem. Chem. Phys. **9**, 1438 (2007).
[5] H. Hagemann and R. O. Moyer, J. Alloys Compd. **330-332**, 296 (2002).
[6] M. M. Barsan, R. O. Moyer Jr., I. S. Butler, and D. F. R. Gilson, J. Alloys Compd. **424**, 73 (2006).
[7] P. Hohenberg and W. Kohn, Phys. Rev. **136**, B864 (1964).
[8] W. Kohn and L. J. Sham, Phys. Rev. **140**, A1133 (1965).
[9] R. G. Parr and W. Yang, *Density-Functional Theory of Atoms and Molecules* (Oxford University Press, New York, 1989).
[10] J. P. Perdew and Y. Wang, Phys. Rev. B **45**, 13244 (1992).
[11] J. P. Perdew, K. Burke, and M. Ernzerhof, Phys. Rev. Lett. **77**, 3865 (1996).
[12] J. P. Perdew, K. Burke, and M. Ernzerhof, Phys. Rev. Lett. **78**, 1396(E) (1997).
[13] X. Gonze *et al.*, Z. Kristallogr. **220**, 558 (2005).
[14] X. Gonze *et al.*, Comput. Mater. Sci. **25**, 478 (2002).
[15] ABINIT code, a common project of the Université Catholique de Louvain, Corning Incorporated, the Université de Liège, the Commissariat à l'Energie Atomique, Mitsubishi Chemical Corp., the Ecole Polytechnique Palaiseau, and other contributors (URL http://www.abinit.org).
[16] S. Goedecker, SIAM J. Sci. Comput. (USA) **18**, 1605 (1997).
[17] M. C. Payne, M. P. Teter, D. C. Allan, T. A. Arias, and J. D. Joannopoulos, Rev. Mod. Phys. **64**, 1045 (1992).
[18] X. Gonze, Phys. Rev. B **54**, 4383 (1996).
[19] N. Troullier and J. L. Martins, Phys. Rev. B **43**, 1993 (1991).
[20] M. Fuchs and M. Scheffler, Comput. Phys. Commun. **119**, 67 (1999).
[21] S. G. Louie, S. Froyen, and M. L. Cohen, Phys. Rev. B **26**, 1738 (1982).
[22] H. J. Monkhorst and J. D. Pack, Phys. Rev. B **13**, 5188 (1976).
[23] X. Gonze, Phys. Rev. B **55**, 10337 (1997).
[24] X. Gonze and C. Lee, Phys. Rev. B **55**, 10355 (1997).
[25] M. I. Aroyo, A. Kirov, C. Capillas, and J. M. P.-M. an H. Wondratschek, Acta Crystallogr., Sect. A: Found. Crystallogr. **A62**, 115 (2006).
[26] R. Lindsay, R. O. Moyer, and D. F. Storey, Z. Phys. Chem., Neue Folge **163**, 309 (1988).
[27] S. F. Parker, K. P. J. Williams, M. Bortz, and K. Yvon, Inorg. Chem. **36**, 5218 (1997).
[28] R. O. Moyer, Jr., J. R. Wilkins, and P. Ryan, J. Alloys Compd. **290**, 103 (1999).
[29] P. Vinet, J. H. Rose, J. Ferrante, and J. R. Smith, J. Phys.: Condens. Matter **1**, 1941 (1989).
[30] R. O. Moyer, Jr., C. Stanitski, J. Tanaka, M. I. Kay, and R. Kleinberg, J. Solid State Chem. **3**, 541 (1971).
[31] R. Gaudoin and W. M. C. Foulkes, Phys. Rev. B **66**, 052104 (2002).
[32] See EPAPS Document No. E-PRBMDO-76-019725 for the linear dependences of the frequencies on the cell parameter *q* and on the pressure *p* summarized in Table S1. For more information on EPAPS, see http://www.aip.org/pubservs/epaps.html.